Original Article

Histological study on the detrimental influences of white LED light on the retina of adult albino rat and the potential effect of simultaneous nicotine administration with highlighting their possible mechanisms

Eman A. Farag, Marwa M. Yousry, Abeer I. Omar

Histology Department, Faculty of Medicine, Cairo University, Cairo, Egypt

ABSTRACT

Background: Light-emitting diodes (LED), the most effective and economic artificial source of light, proved to emit more blue light than traditional sources even the most popular white LED light. Blue light had many health problems as light-retinal damage. Nicotine, one of the main solid of cigarette smoke, caused end organ damage and promoted retinal lesions through different mechanisms.

Aim of the work: Investigating the possible retinal changes induced by domestic white LED light in albino rat and the probable impact of nicotine on these changes with highlighting their possible mechanisms.

Materials and Methods: Forty-two adult male albino rats were equally divided into three groups; control (I), LED (II) & Nicotine-LED (III). Groups II and III were kept in 5 days normal light/dark cycle, 14 days darkness then normal cycle with domestic white LED light for 9 days. Additionally, rats of group III received daily oral nicotine (3 mg /day) for 28 days (experimental duration). All rats were sacrificed at the end of the experiment and superoxide anion (O_2^-) level was measured in the retinal homogenates of each group. Retinal sections from all groups were subjected to toluidine blue, H&E and immunohistochemical stains for caspase-3, vimentin and inducible nitric oxide synthase (iNOS). Area percent of positive reactions, thickness of outer and inner nuclear layers and number of ganglion cells were measured. The obtained data is then statistically analyzed.

Results: Features of retinal damage and increased O_2^- level were detected in both groups II and III with marked injury in group III. Studying group III immunohistochemically, revealed marked increase in vimentin and iNOS and significant decrease in caspase-3 positive reactions versus group II.

Conclusions: White LED light could result into deleterious retinal damage which could be exaggerated by nicotine, a main component of cigarette smoke, and rapidly progressed to age related macular degeneration.

Key Words: LED, nicotine, retina, vimentin, iNOS and caspase-3

Revised: 17 May 2017, **Accepted:** 20 May 2017

Corresponding Author: Eman Abas Farag, **Tel.:** 01140639636, **E-mail:** dr.emanabas@yahoo.com; emanabas@kasralainy.edu.eg, Histology Department, Faculty of Medicine, Cairo University, Cairo, Egypt

ISSN: 1110-0559, September Vol. 40, No. 3

INTRODUCTION

Light-emitting diodes (LED) is one of the artificial lighting sources. It was manufactured for domestic use as it emitted all of its energy within the human visible wavelength range. Thus regarding light energy production and energy saving, LED light was considered to be the most effective and economic artificial source of light[1]. LED was proved to emit much more blue light than traditional light sources[2]. Such short wavelength blue light (460 - 500 nm) had many health problems such as circadian rhythm disturbance[1] and light induced retinal damage that might progress to age related macular degeneration (AMD)[2]. This hazardous blue light was even produced by the most popular white LED source called phosphor-conversion (PC) LED. As it was formed of LED chip radiating blue light that passed through a yellow phosphor coat to produce the ultimate normal white light to human eye[3].

Cigarette smoke composed of more than 4000 chemicals in solid and gaseous forms. Nicotine and tar were the main solid components while carbon monoxide, carbon dioxide and nitric oxide represented the major gaseous components[4]. These toxic components were proved to cause end-organ damage through their direct toxic effects on the tissues, immune system activation, hypoxia induced by pulmonary lesion and induction of vascular lesions[5].

In addition, smoking was considered as a major predisposing factor for the development of retinal lesions, especially age related macular degeneration (AMD)[6]. The incidence of wet AMD was increased two to four folds by smoking[5] and decreased in former smokers by 50% than current smokers[7]. This might occur due to lesion of the retinal pigmented epithelium (RPE) induced by a toxic component in tobacco smoke called benzopyrene[8].

 DOI: 10.21608/EJH.2017.4659

Nicotine, one of the particulate chemicals in cigarette smoke, was proved to be one of the most toxic components in cigarette smoke[9] through induction of oxidative stress and angiogenesis[10].

This study aimed to investigate the possible retinal changes induced by domestic white LED light in albino rat and the probable impact of nicotine (a main component of cigarette smoke) on these changes, together with emphasizing their possible mechanisms.

MATERIAL AND METHODS

I)Animals:

Forty two adult male albino rats (180 - 200g) were used in this study. They were housed in the laboratory animal house unit of Kasr Al-Aini, Faculty of Medicine, Cairo University. The rats were treated according to the guidelines approved by the Animal Use Committee of Cairo University. All rats were kept under the same environmental conditions where they were provided with ordinary rat chow and water ad libitum. They were housed at 24 ± 1°C in normal light/dark cycle (12 hours light/12 hours dark).

II)Materials:

- White PC LED light of 6500 K correlated color temperature (CCT) purchased from Venus Lighting Limited, Foshan city, Guangdong China (item No. A60-12W-E27).

- (S)-(-)-Nicotine 99% (C10H14N2) was purchased from Alfa Aesar Thermo Fisher company, Jermany, product no. A12398. It was supplied as liquid form (25 g/ bottle).

III)Experimental design:

The rats were divided into three groups, 14 rats each:

Control group (group I):

The rats were kept in complete darkness throughout the whole experimental duration (28 days).

LED group (group II):

Animals were kept in normal light/dark cycle for 5 days followed by 14 days darkness to allow retinal recovery from light exposure in their former environment. Then they were subjected to 9 days of light/dark cycle using white PC LED light[11].

Nicotine - LED group (group III):

The rats were treated as in group II in addition to simultaneous oral administration of nicotine throughout the whole duration (28 days). Nicotine was handled very carefully due to its high toxicity and mixed with drinking water (200 µg/ml) in a foil covered bottle due to its light sensitivity. Based on that each rat drank 15 – 20 ml of the mixture daily so, each rat received at least 3 mg nicotine/ day for 4 weeks. Drinking the least dose of nicotine was ensured by certifying the amount of water drunk/rat/day. This dose was adjusted to reach the serum nicotine level of chronic moderate smokers at the end of the experiment[12].

Experimental procedure:

1-Light exposure:

Un-anesthetized rats with undilated pupils were housed in transparent plastic cages. Each cage contained just one rat to ensure proper light exposure. Drinking water was supplied by a bottle attached to the side of each cage to avoid obstruction between the light and the animal. Each cage was placed in the center of a rack shelf with 35 cm between each shelf and the other. The light sources were fixed at the top of each shelf 20 cm away from each other to provide the rats with the common domestic illumination level (750 lux). Light exposure started from 6.00 PM to 6.00 AM to match the human nocturnal activity pattern[11].

2- The animals of the three groups were sacrificed after 28 days in the animal house, Faculty of Medicine, Cairo University. Just before scarification the animals were anesthetized with intraperitoneal injection of ketamine (90 mg/kg)/xylazine (15 mg/kg)[13]. Both eyeballs of each rat were enucleated.

3-*Biochemical investigation:*

The eyeballs of six rats from each group were used for the biochemical analysis. Each eyeball was incised behind the limbus to separate the anterior and the posterior eye poles. The retina was separated, kept in microtube and homogenized[14]. Retinal homogenates of each group were used to measure superoxide anion (O_2-), one of the reactive oxygen species used as oxidative stress marker, at the Biochemistry Department, Faculty of Medicine, Cairo University according to the previously reported methodology[15].

Light microscopic studies:

A) The right eyeballs of the remaining eight rats of each group were fixed in 10% formol saline and kept for 24 hours then processed to obtain Paraffin blocks. Paraffin sections 6 micrometers thick were cut and stained by:

- Hematoxylin and Eosin stain[16].

- Immunohistochemical staining for:

1. Caspase-3 antibody: It is a rabbit polyclonal antibody (Lab Vision Corporation Laboratories, catalogue number PA1-26426).

2. Vimentin antibody: It is a mouse monoclonal antibody (Lab Vision Corporation Laboratories, catalogue number MA5-11883).

3. iNOS (inducible Nitric Oxide Synthase) antibody: It is a rabbit polyclonal antibody (Lab Vision Corporation Laboratories, catalogue number PA1-036).

Immunostaining required pretreatment[17], this was done by boiling for 10 minutes in 10Mm citrate buffer (cat no AP 9003) pH 6 for antigen retrieval and leaving the sections to cool in room temperature for 20 minutes. Then, the sections were incubated for one hour with the primary antibodies. Immunostaining was completed by the use of Ultravision detection system (cat no TP - 015- HD). Counterstaining was done using Mayer's hematoxylin (cat no TA- 060- MH). Primary antibodies, citrate buffer, Ultravision detection system and Mayer's hematoxylin were purchased from Labvision Thermoscientific USA.

The left eyeballs of the remaining eight rats of each group were immediately put in 2.5 % ice-cold glutaraldehyde for 30 minutes. The retina of each eyeball was separated and cut into small pieces. These specimens were prefixed in 2.5 % glutaraldehyde for 2 hours then postfixed in 1% osmium tetroxide in 0.1M phosphate buffer at pH 7.4 and 4 °C for 2 hours. The fixed specimens were dehydrated and embedded in resin[18]. Semithin sections (1µm thick) were cut and stained with 1% toluidine blue[19].

4-Morphometric study:

It included measuring of:

- Mean area percent of caspase-3 immuno-expression in caspase-3 immunostained sections at a magnification of ×400.
- Mean area percent of vimentin immuno-expression in vimentin immunostained sections at a magnification of ×200.
- Mean area percent of iNOS immuno-expression in iNOS immunostained sections at a magnification of ×400.
- Thickness of outer and inner nuclear layers in H. & E. stained sections at a magnification of ×400.
- Mean number of ganglion cells in ganglion cell layer in H. & E. stained sections at a magnification of ×400.

All measurements were done in 10 non overlapping fields from different sections of eight animals of each group which were subjected to H. & E. and immunohistochemical staining. The area percent was calculated. Image analysis was done using Leica microsystems LTD (DFC 295) software image analysis computer system (Germany) in Dentistry Research and Equipment Unit, Faculty of Dentistry, Cairo University.

5-Statistical analysis:

The morphometric and biochemical measurements were expressed as mean ± standard deviation (SD) and were analyzed statistically using the software "Statistics for windows SPSS" version 16. This was done using one-way analysis of variance ANOVA followed by "Tuckey" post hoc test. Results were considered significant when P value was < 0.05[20].

RESULTS

No deaths were observed in the rats during the experiment.

Biochemical results and statistical analysis:

The mean value of superoxide anion (O_2^-) in retinal homogenates was significantly increased in group III when compared to that of group II "significant $P< 0.05$" (Table 1).

Light microscopic results:

Hematoxylin and Eosin stain:

Control group (group I):

Sections of control rats showed normal histological structure of the retinal layers. The photoreceptor layer appeared with an outer lightly stained segment formed of parallel processes (outer segment) and an inner densely stained segment (inner segment). The outer limiting membrane appeared as an acidophilic line separating between photoreceptor layer and the rest of the retinal layers. The outer nuclear layer formed of multiple regularly arranged rows of rod cells' nuclei that appeared small, multiple and dark and some cone cells' nuclei which were larger, fewer and lighter than that of rod cells. They also showed the outer plexiform layer that had a reticular appearance and the inner nuclear layer which seemed to be thinner with larger and paler nuclei with variable shape, size and density than those of the outer nuclear layer. The inner plexiform layer appeared with the same reticular appearance of the outer plexiform layer, but thicker. The ganglion cell layer appeared formed of one row of large rounded widely separated cells with larger and paler nuclei than those of the other nuclear layers. In-between these cells there were glial cells (astrocytes) with darker nuclei. The nerve fiber layer appeared consisting of the axons of the ganglion cells (Figs. 1-3).

LED group (group II):

Examination of the retinal sections after 9 days of exposure to domestic white LED light revealed features

of retinal damage where the photoreceptor layer was disorganized and vacuolated. The outer limiting membrane was interrupted and there were multiple empty spaces in the outer and inner nuclear layers. In addition, there were thinning and disruption of the outer plexiform layer. The ganglion cell layer showed few ganglion cells, some darkly stained glial cells and congested blood vessel (Fig. 4).

***Nicotine - LED group (group III)*:**

Retinal sections examination after 9 days of exposure to domestic white LED light with concomitant administration of nicotine for 4 weeks showed exaggeration of retinal damage. As, there was nearly absent photoreceptor and outer plexiform layer with marked disruption of the outer limiting membrane. Additionally, multiple empty spaces appeared within the outer and inner nuclear layers. The ganglion cell layer revealed markedly congested blood vessel, very few shrunken and irregular ganglion cells and multiple glial cells (Fig. 5).

Semithin sections:

Control group (group I):

Control rats' retinal sections demonstrated normal histological structure of the retina where it was formed of ten layers. The retinal pigmented epithelium appeared formed of one layer of cuboidal cells with cytoplasmic vacuolations and central pale rounded nuclei with prominent nucleoli. The photoreceptor layer was formed of parallel well organized outer and inner segments. The outer limiting membrane appeared as a continuous dark line just below photoreceptor layer. The outer nuclear layer composed of cell bodies of both rods and cones where rods' nuclei are more numerous, darker and smaller than that of cones. The outer plexiform layer showed thin reticular appearance between outer and inner nuclear layers. In addition, there were appearance of nuclei of four types of cells in inner nuclear layer which were larger than those of rods and cones. They were bipolar cells (most numerous and widely distributed with oval to rounded nuclei of moderate density), Müller cells (scattered in-between bipolar cells with angled darkly stained nuclei) and horizontal and amacrine cells (large rounded pale stained nuclei on the outer and inner boundaries of inner nuclear layers, respectively). The inner plexiform layer was thicker than the outer one and had a reticular appearance. The ganglion cell layer was formed of one raw of ganglion cells (widely separated with pale nuclei and prominent nucleoli, their nuclei were the largest among the three nuclear layers of the retina). In between the ganglion cells there were astrocytes (cells with darkly stained nuclei). Moreover, there was appearance of the nerve fiber layer (axons of ganglion cells) and inner limiting membrane (darkly stained continuous line) (Figs. 6-9).

***LED group (group II)*:**

After 9 days of exposure to domestic white LED light, the retinal sections revealed disorganization and vacuolation of the photoreceptor layer and remnants of the outer limiting membrane. The retinal pigmented epithelium showed shrunken cells with deeply stained cytoplasm and darkly stained shrunken irregular nuclei. Multiple empty spaces, shrunken and fragmented nuclei appeared in the outer and inner nuclear layers. There were disruption of the outer plexiform layer and thickened Müller processes in the inner plexiform layer. The ganglion cell layer revealed few ganglion cells where some of them had irregular or dark nuclei in addition to the presence of astrocytes. The inner limiting membrane was apparently normal (Figs. 10-13).

Nicotine - LED group (group III):

Examination of retinal sections of this group disclosed complete absence of photoreceptor layer, outer limiting membrane and outer plexiform layer. The retinal pigmented epithelium appeared with few cells which were either shrunken irregular cells with pyknotic nuclei and/or swollen cells with absent nuclei and cytoplasmic vacuolations. The outer nuclear layer is formed of 1-2 layers of cell bodies surrounded by multiple empty spaces. Most of these cell bodies showed cytoplasmic vacuolations and shrunken nuclei. The inner nuclear layer showed multiple empty spaces, some irregular nuclei and some shrunken darkly stained nuclei. The ganglion cell layer revealed few irregular and/or shrunken ganglion cells together with astrocytes and congested blood vessels. There was apparently normal inner limiting membrane (Figs. 14 & 15).

Immunohistochemical results:

•Immunohistochemical staining for caspase-3:

Control group (group I):

Examination of the retinal sections revealed absence of caspase-3 positive immunoreaction in all nuclear layers of the retina (outer and inner nuclear and ganglion cell layers) (Fig. 16).

LED group (group II):

Retinal sections of this group showed caspase-3 positive immunoreactivity in some cells of the outer and inner nuclear layers and few cells in the ganglion cell layer (Fig 17).

Nicotine - LED group (group III):

There was positive caspase-3 immunoreaction in few cells of the outer and inner nuclear layers and very few cells in the ganglion cell layer (Fig 18).

•Immunohistochemical staining for vimentin:

Control group (group I):

Examination of the retinal sections reflected positive vimentin immunoreaction limited to the Müller cells' thin processes in the inner retina and astrocytes' cytoplasm and processes in the ganglion cell layer only (Fig. 19).

LED group (group II):

Vimentin positive immunoreactivity appeared in Müller cells' cytoplasm and their thickened processes that seemed extending towards the outer limiting membrane in addition to the astrocytes' cytoplasm and processes around the congested blood vessels in the ganglion cell layer (Fig 20).

Nicotine - LED group (group III):

Strong abundant positive immunoreaction for vimentin in cytoplasm of Müller cells and their thickened processes appeared extending through the whole retinal layers and replacing the outer limiting membrane. Additionally, there was positive reaction for vimentin in astrocytes' cytoplasm and their thickened processes around the congested blood vessels in the ganglion cell layer (Fig 21).

•Immunohistochemical staining for iNOS:

Control group (group I):

iNOS positive immunoreactivity was undetectable in all layers of retinal sections of this group (Fig 22).

LED group (group II):

Retinal sections of this group revealed positive iNOS immunoreaction in inner nuclear and ganglion cell layers (Fig 23).

Nicotine - LED group (group III):

In this group, iNOS immunoreactivity extended to the outer nuclear layer in addition to its presence in the inner nuclear and ganglion cell layers (Fig 24).

Morphometric results (Table 1):

Mean thickness of the outer and inner nuclear layers and mean number of ganglion cells in ganglion cell layer showed significant decrease in LED group versus control. Moreover, Nicotine - LED group represented a significant decrease compared to LED group "significant *P< 0.05*".

Regarding the mean area percent of vimentin positive immunostaining, the retinal sections of LED group recorded significant increase versus the control group. Additionally, there was significant increase in the Nicotine - LED group than in the LED group "significant *P< 0.05*".

The mean area percent of iNOS positive immunostaining in retinal sections of Nicotine - LED group showed significant increase than that of the LED group "significant *P< 0.05*". However, the mean area percent of caspase-3 positive immunostaining was significantly decreased in group III when compared to that of group II "significant *P< 0.05*".

Table (1): Mean value ± SD of biochemical & morphometric parameters in all studied groups:

Parameters	Group I	Group II	Group III
Mean value of O_2^- nmol/mg tissue	undetectable	0.58±0.073	1.01±0.13□
Mean numbers of ganglion cells	13.8±1.6	7.6±1.26*	2.8±0.7*□
Mean thickness of the outer nuclear layer	324.14±6.22µm	175.4±6.08µm*	87.9±6.27µm*□
Mean thickness of the inner nuclear layer	253.8±9.8µm	135.5±9.18µm*	79.9±4.28µm*□
Mean area % of vimentin	0.735±0.057	2.6±0.6*	4.2±0.9*□
Mean area % of iNOS	undetectable	0.77±0.06	1.26±0.05□
Mean area % of caspase-3	undetectable	1.08±0.13	0.56±0.08□

* Significant (P < 0.05) as compared to group I.
□ Significant (P < 0.05) as compared to group II.

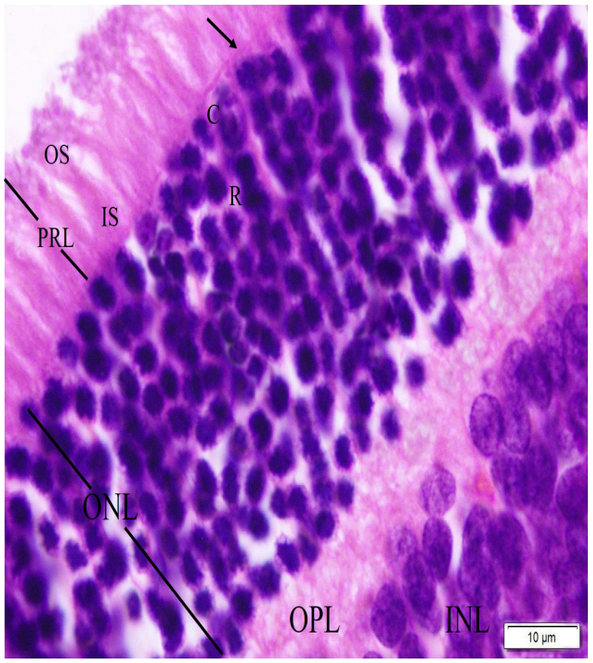

Fig. 1: A photomicrograph of a section in the retina of group I (control group) showing normal histological structure of the retinal layers. PRL is composed of lightly stained OS and densely stained IS. An acidophilic line, OLM (arrow) separates PRL from the rest of the retinal layers. ONL consists of multiple regularly arranged rows of small dark nuclei of rod cells (R) and fewer larger and lighter nuclei of cone cells (C). OPL exhibits reticular appearance. Part of INL appears with larger and paler nuclei. (H&E, x1000).

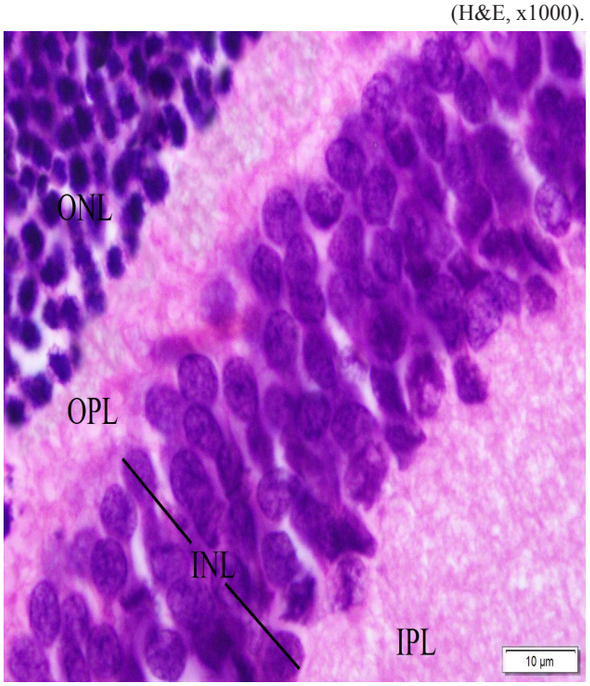

Fig. 2: A photomicrograph of a section in the retina of group I illustrating INL that appears thinner with larger and paler nuclei with different shape, size and density than those of the ONL. Moreover, there is a part of ONL, OPL and IPL with normal histological appearance. (H&E, x1000).

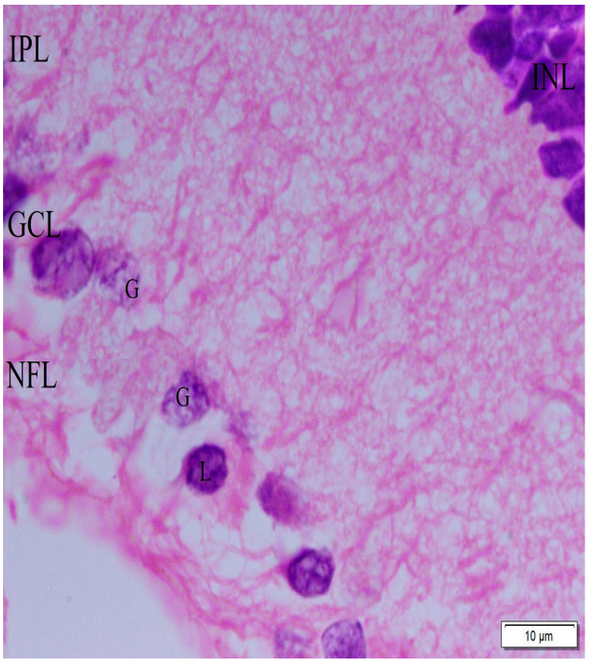

Fig. 3: A photomicrograph of a section in the retina of group I showing IPL with the same reticular appearance of the OPL, but thicker. GCL is formed of one row of large rounded widely separated ganglion cells (G) with large pale nuclei. Glial cells (L) with darker nuclei are seen in-between the ganglion cells. NFL consisting of axons of the ganglion cells can be noted. Small area of INL can be also seen. (H&E, x1000).

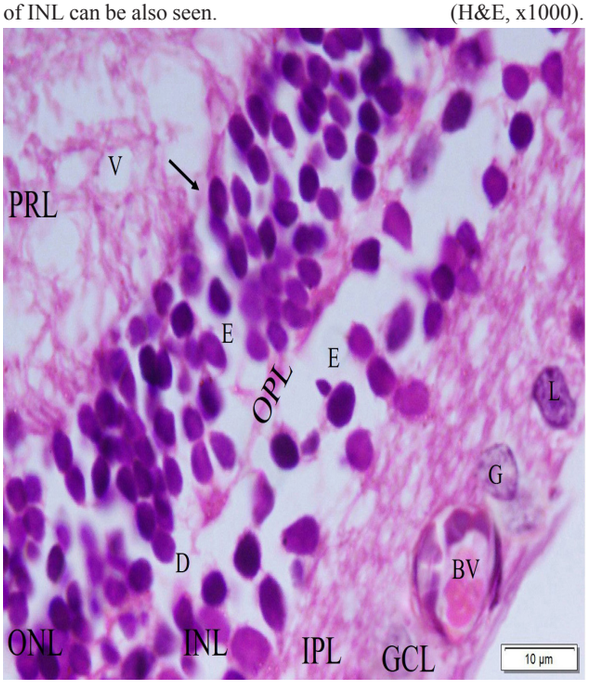

Fig. 4: A photomicrograph of a section in the retina of group II (LED group) illustrating disorganized and vacuolated PRL (V), interruption of OLM (arrow) and multiple empty spaces (E) in the ONL & INL. OPL appears thinned and disrupted (D). Few ganglion cells (G), some darkly stained glial cells (L) and congested blood vessel (BV) are observed in the GCL. (H&E, x1000).

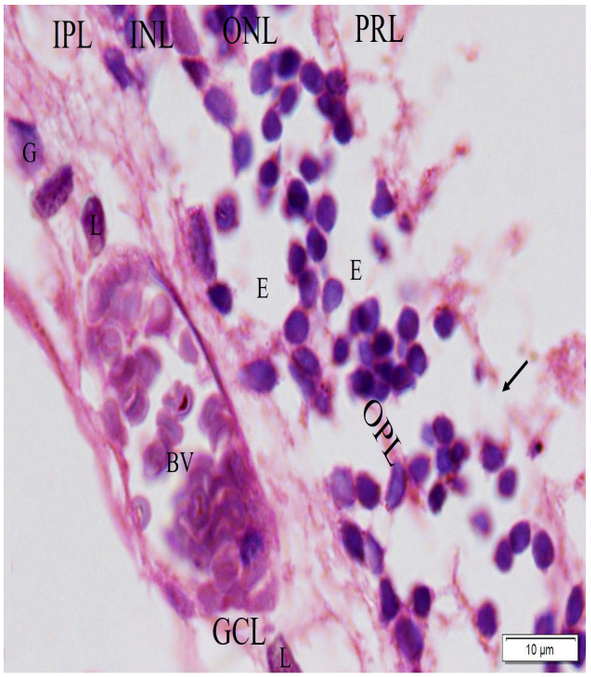

Fig. 5: A photomicrograph of a section in the retina of group III (Nicotine - LED group) showing nearly absent PRL and OPL with marked disruption of the OLM (arrow). Moreover, ONL & INL exhibit multiple empty spaces (E). Markedly congested blood vessel (BV), very few shrunken and irregular ganglion cells (G) and multiple glial cells (L) can be seen in the GCL. (H&E, x1000).

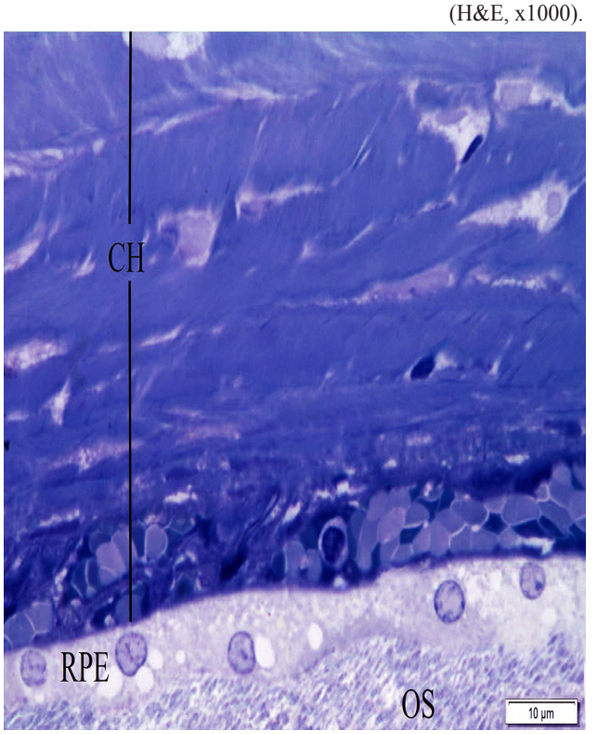

Fig. 6: A photomicrograph of a section in the retina of group I (control group) illustrating the choroid (CH), RPE and OS of PRL. RPE is formed of cuboidal cells with cytoplasmic vacuolations and central pale rounded nuclei with prominent nucleoli. (Toludine blue, x1000).

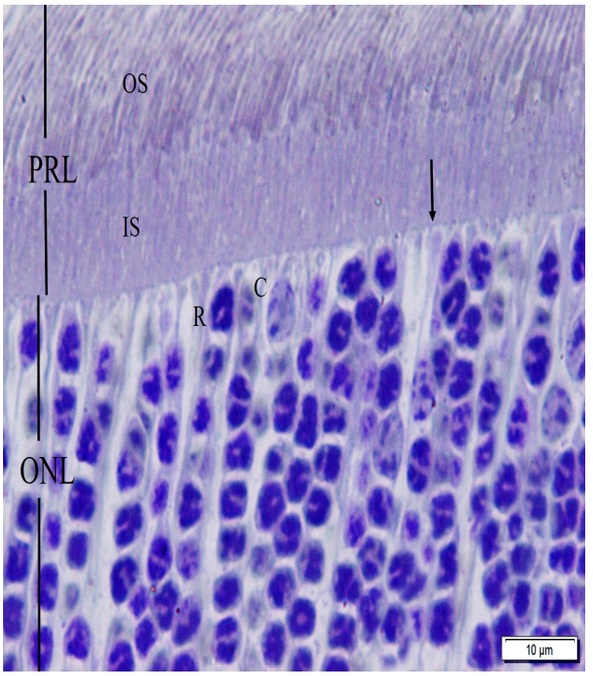

Fig. 7: A photomicrograph of a section in the retina of group I (control group) showing parallel well organized OS and IS of the PRL. The OLM appears as a continuous dark line (arrow) just below PRL. ONL shows nuclei of rod cells (R) that appear dark and numerous and cone cells (C) which are larger. (Toludine blue, x1000).

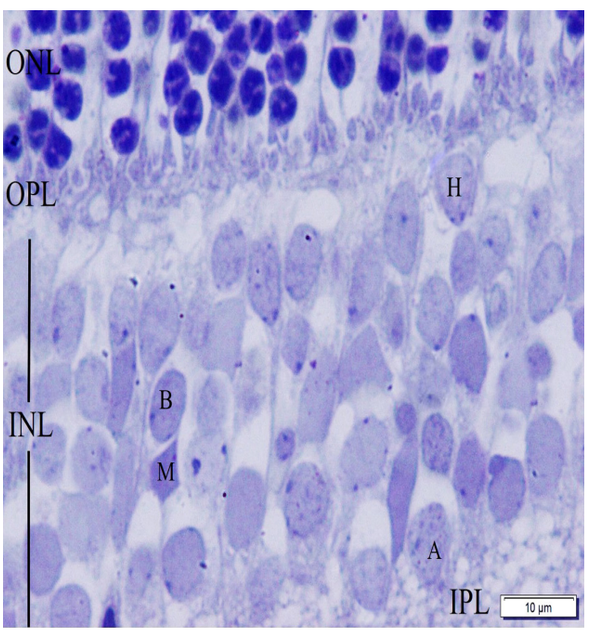

Fig. 8: A photomicrograph of a section in the retina of group I illustrating OPL with thin reticular appearance between ONL & INL. The INL is formed of four types of cells; B cells, the most numerous with oval to rounded nuclei of moderate density. M cells have angled deeply stained nuclei between bipolar cells. H and A cells appear with large rounded lightly stained nuclei on the outer and inner boundaries of INL, respectively. Note the presence of a part of IPL. (Toludine blue, x1000).

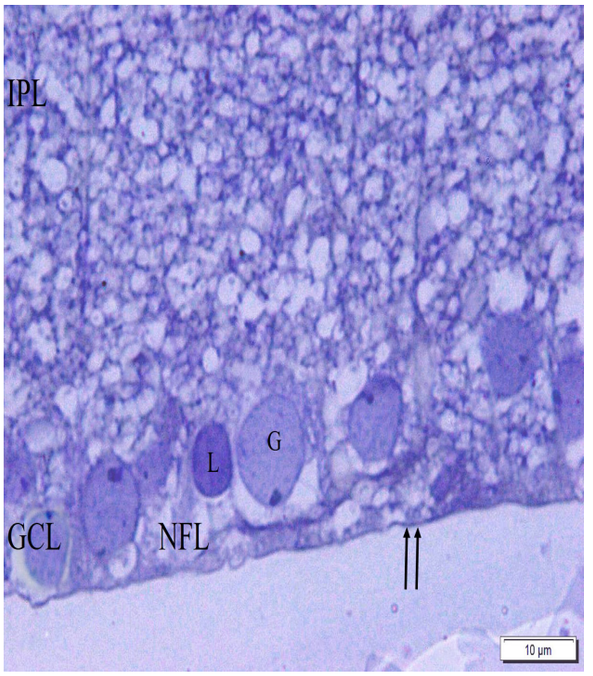

Fig. 9: A photomicrograph of a section in the retina of group I showing the reticular appearance of IPL which is thicker than the outer one. One raw of pale nuclei with prominent nucleoli of ganglion cells (G) and darkly stained nuclei of astrocytes (L) are observed in the GCL. NFL and ILM, a darkly stained continuous line (double arrows) can be noted. (Toludine blue, x1000).

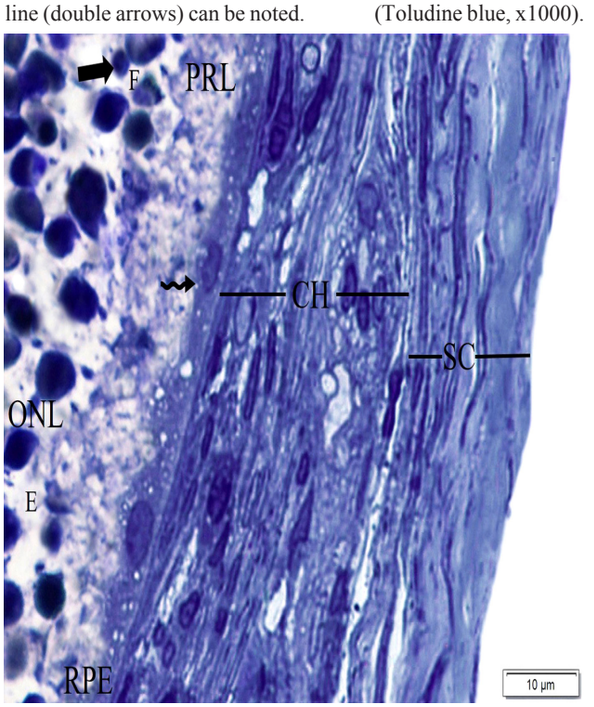

Fig. 10: A photomicrograph of a section in the retina of group II (LED group) demonstrating the sclera (SC), choroid (CH), RPE and PRL. RPE with shrunken cells, deeply stained cytoplasm and darkly stained shrunken irregular nuclei (wavy arrow) are clearly observed. Part of ONL exhibits empty spaces (E), shrunken (thick arrow) and fragmented (F) nuclei. (Toludine blue, x1000).

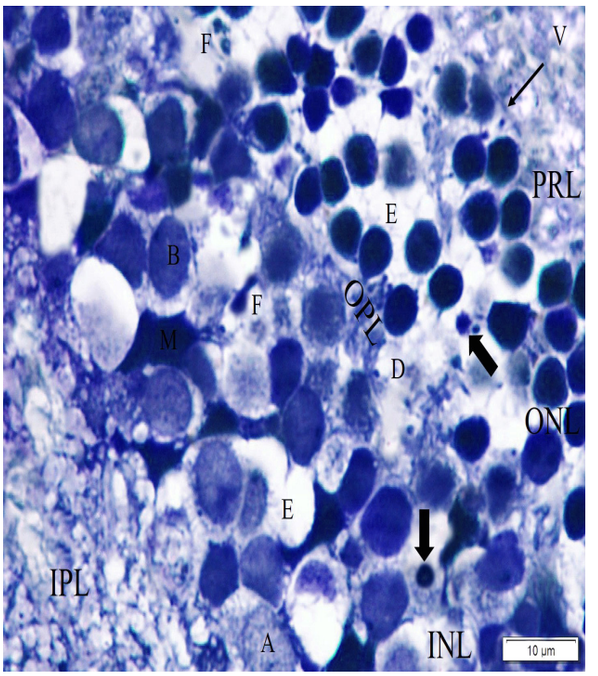

Fig. 11: A photomicrograph of a section in the retina of group II (LED group) illustrating disorganization and vacuolation of the PRL (V) and remnants of the OLM (arrow). ONL & INL show multiple empty spaces (E), shrunken (thick arrow) and fragmented (F) nuclei. Disrupted OPL (D) and a part of IPL are also noted. Notice the presence of B, M and A cells in INL. (Toludine blue, x1000).

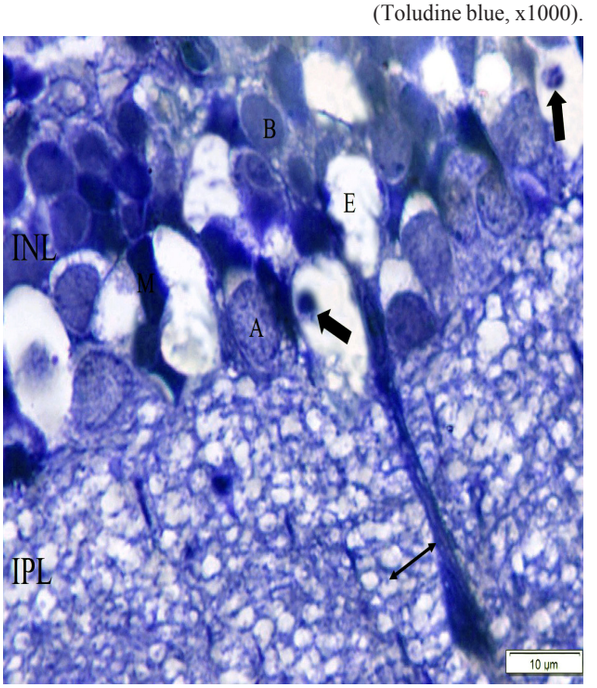

Fig. 12: A photomicrograph of a section in the retina of group II illustrating empty spaces (E) and shrunken nuclei (thick arrow) in INL and thickened Müller processes (double headed arrow) in the IPL. Note the presence of apparently normal B, M and A cells in INL. (Toludine blue, x1000).

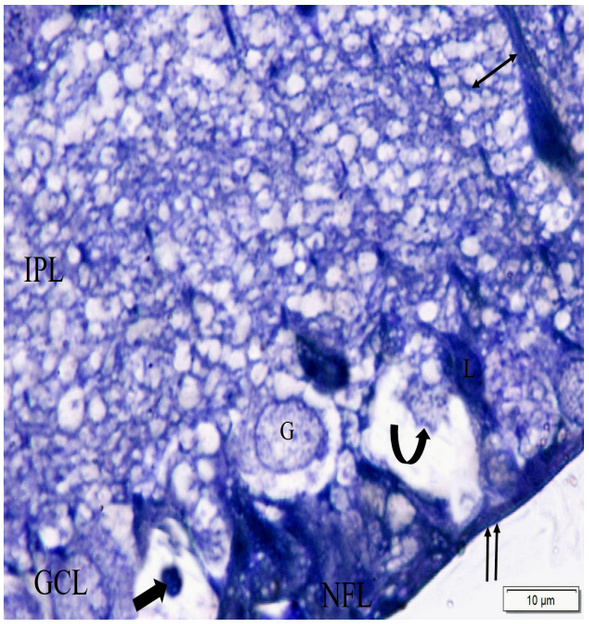

Fig. 13: A photomicrograph of a section in the retina of group II showing GCL with few ganglion cells (G) where some of them with irregular (curved arrow) or shrunken nuclei (thick arrow) and astrocytes (L). Notice the presence of thickened Müller processes (double headed arrow) in the IPL. NFL and apparently normal ILM (double arrows) can be seen. (Toludine blue, x1000).

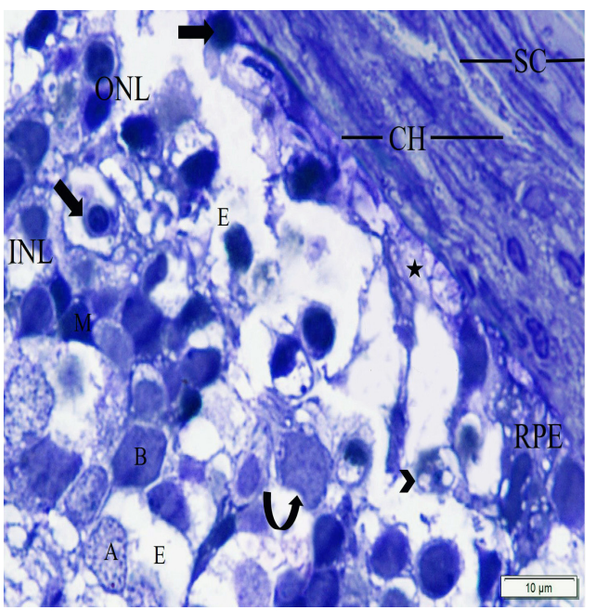

Fig. 14: A photomicrograph of a section in the retina of group III (Nicotine - LED group) demonstrating RPE that show few cells with either shrunken irregular cells with pyknotic nuclei (thick arrow) and/or swollen cells with absent nuclei and cytoplasmic vacuolations (star). Complete loss of PRL, OLM and OPL is clearly observed. Note the presence of 1-2 layers of cell bodies of ONL surrounded by multiple empty spaces (E) where most of them exhibit cytoplasmic vacuolations and shrunken nuclei (arrow head). In addition, the INL shows multiple empty spaces (E), some irregular nuclei (curved arrow) and some shrunken darkly stained nuclei (thick arrow). Note the presence of B, M and A cells of INL in addition to parts of the choroid (CH) and sclera (SC). (Toludine blue, x1000).

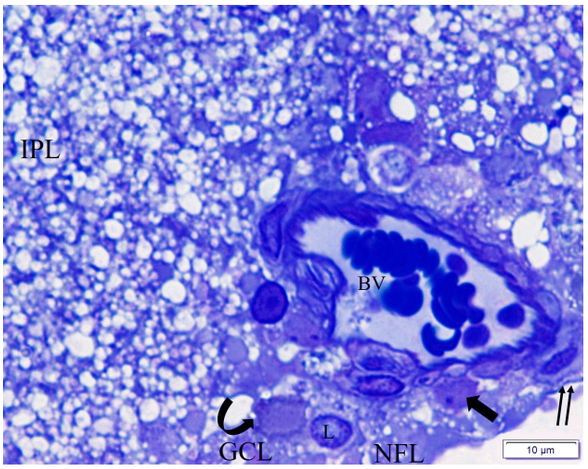

Fig. 15: A photomicrograph of a section in the retina of group III illustrating few irregular (curved arrow) and/or shrunken (thick arrow) ganglion cells together with astrocytes (L) and congested blood vessels (BV) in GCL. IPL, NFL and ILM appear normal (double arrows). (Toludine bluen, x1000).

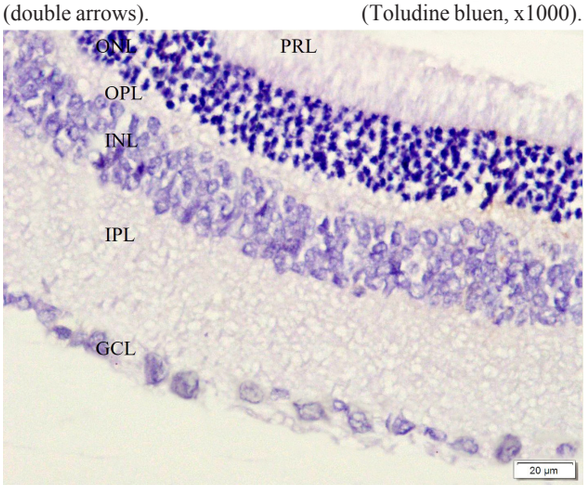

Fig. 16: A photomicrograph of a section in the retina of group I showing absence of caspase-3 positive immunoreaction in all nuclear layers of the retina (ONL, INL & GCL). (Immunohistochemical stain for caspase-3, x400).

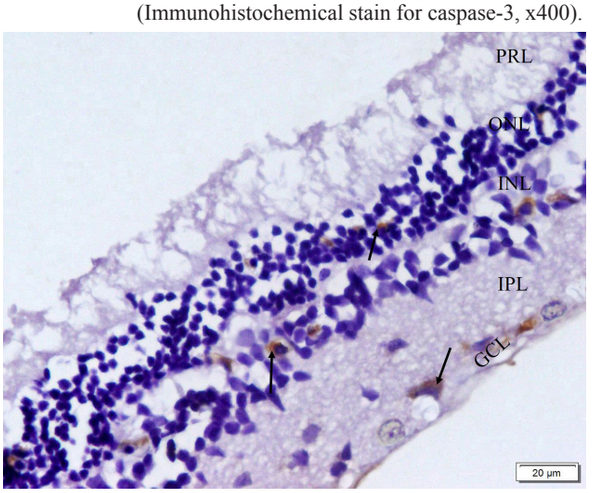

Fig. 17: A photomicrograph of a section in the retina of group II illustrating positive immunoreaction for caspase-3 (arrows) in some cells of the ONL & INL and few cells in the GCL. (Immunohistochemical stain for caspase-3, x400).

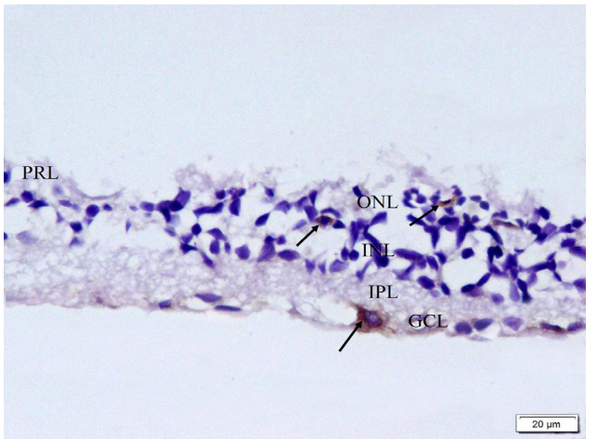

Fig. 18: A photomicrograph of a section in the retina of group III demonstrating caspase-3 positive immunoreactivity (arrows) in few cells of the ONL & INL and very few cells in the GCL. (Immunohistochemical stain for caspase-3, x400).

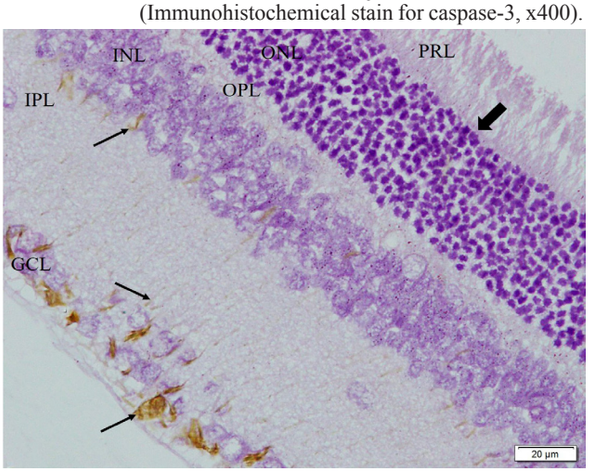

Fig. 19: A photomicrograph of a section in the retina of group I showing positive vimentin immunoreaction (arrows) limited to the Müller cells' thin processes in the inner retina and astrocytes' cytoplasm and processes in the GCL. Note the negative immunoreaction in the OLM (thick arrow). (Immunohistochemical stain for vimentin, x400).

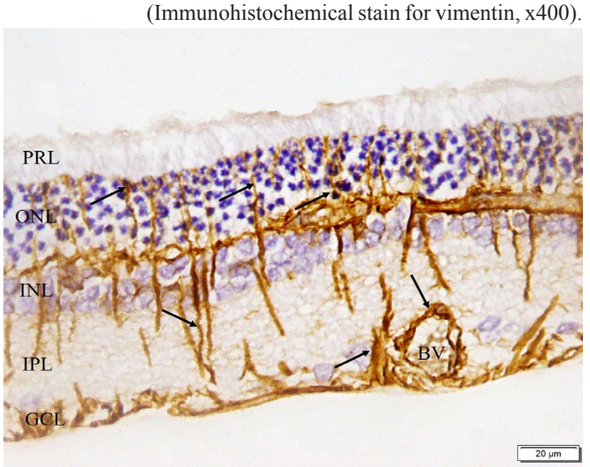

Fig. 20: A photomicrograph of a section in the retina of group II illustrating positive immunoreactivity for vimentin (arrows) in Müller cells and their thickened processes that seemed extending towards the OLM together with positive immunoreaction (arrows) in the astrocytes' cytoplasm and processes around the congested blood vessels (BV) in the GCL. (Immunohistochemical stain for vimentin, x400).

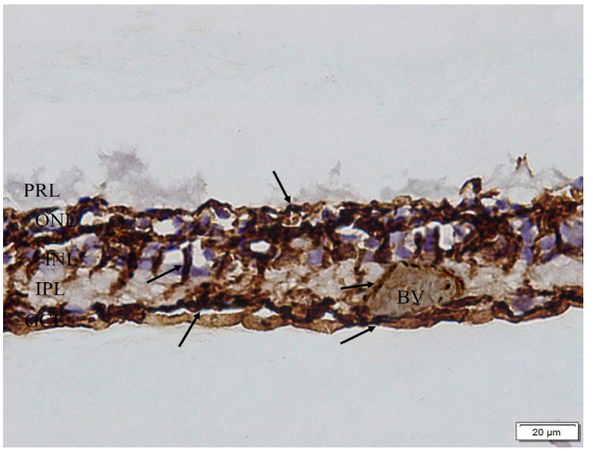

Fig. 21: A photomicrograph of a section in the retina of group III demonstrating strong abundant positive immunoreaction for vimentin (arrows) in Müller cells and their thickened processes that extend through the whole retinal layers and replacing the OLM. Also, astrocytes and their thickened processes around the congested blood vessels (BV) in the GCL exhibit positive reaction for vimentin (arrows). (Immunohistochemical stain for vimentin, x400).

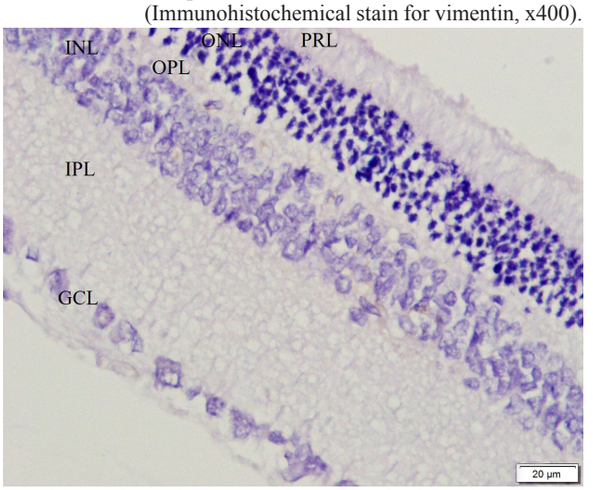

Fig. 22: A photomicrograph of a section in the retina of group I showing undetectable positive immunoreaction for iNOS in all nuclear layers of retinal sections (ONL, INL & GCL). (Immunohistochemical stain for iNOS, x400).

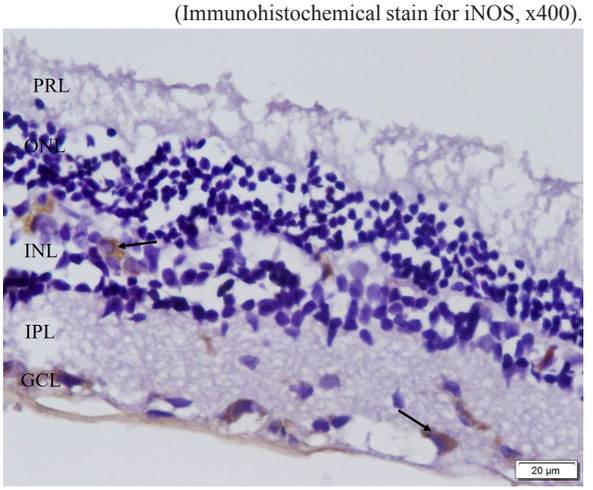

Fig. 23: A photomicrograph of a section in the retina of group II illustrating iNOS positive immunoreaction (arrows) in INL and GCL only. (Immunohistochemical stain for iNOS, x400).

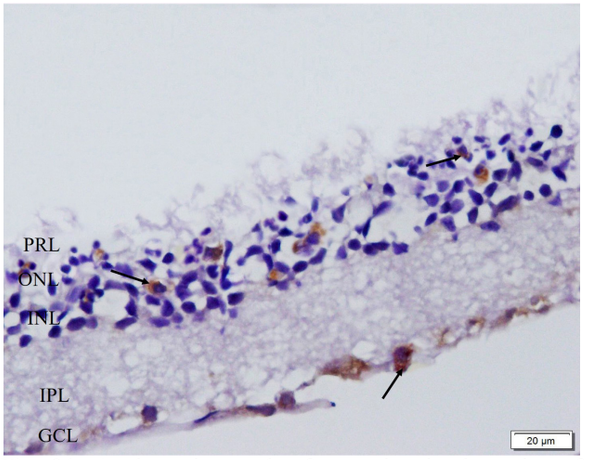

Fig. 24: A photomicrograph of a section in the retina of group III demonstrating iNOS positive immunoreactivity (arrows) extended to the ONL. Additionally there is positive immunoreaction (arrows) in INL and the GCL. (Immunohistochemical stain for iNOS, x400).

DISCUSSION

Artificial lighting, one of the characteristics of civilization and modern life, increases health hazards through light pollution especially with the elaboration of more complicated lighting sources[21]. LED, especially the white LED (PC LED), is one of the artificial lighting sources that is widely used nowadays as it emitted all of its energy within the human visible wavelength range. So it was considered to be the most effective and economic artificial source of light[1].

Albino rats were used in the current work as rats are the best experimental animals to study light-retinal injury[22]. This is based on that the effects of light were more obvious as the rat's retinal irradiance is 60% greater than that of human when using the same light source[11]. Additionally, the use of albino (non-pigmented) rats avoided the controversial effects of melanin present in the retinal pigmented epithelium (RPE)[14]. Melanin might have a retinal protective effect in case of low intensity light through light absorption. So, after moderate lighting for 1 week no retinal histological changes could be observed in pigmented rats contrary to that occurred in albino rats[23]. On the other side, melanin could exaggerate the light retinal injury with high intensity light as it might act as a chromophore generating oxygen free radicals[14]. Moreover, the albino rats used in this study were kept in complete darkness before their exposure to LED light to increase the susceptibility to light-retinal injury more than in normal retinas[24] by allowing retinal recovery from light exposure in the former environment[11].

In group II of the current study, 9 days exposure to the common domestic illumination level (750 lux) of white PC LED light with normal light/dark cycle resulted into numerous empty spaces and some shrunken or fragmented nuclei in the outer nuclear layer (ONL) with significant decrease in its thickness than control group. This finding could be explained by apoptotic cell death reported to occur by other researchers in a previous study[11] after LED light exposure. They stated the presence of nuclear condensation and fragmentation in ONL with marked decrease in the number of its rows to become 4-5 instead of 10-14 in control retinas. Such apoptotic cell death could be supported in the present study by positive caspase-3 immunoreaction in ONL compared to the undetected reaction in control group.

Death of the photoreceptors might explain the disorganization and vacuolations detected in the photoreceptor layer (PRL) of this group. These findings are similarly reported in a former study[11] where electron microscopic pictures revealed disruption and swelling of the inner and outer segments of PRL following LED exposure. Furthermore, it might result into disruption of the tight junctions between their inner segments and the peripheral processes of Müller cells[25]. This in turn, could explain interruption of the outer limiting membrane (OLM) detected in this group. Additionally, photoreceptors death could explain the presence of multiple empty spaces, fragmented and shrunken nuclei in inner nuclear layer (INL), positive caspase-3 immunoreaction of some of its cells and the significant decrease in its thickness in this group versus control group. This occurred through post synaptic cellular death where there was synaptic loss with subsequent loss of the trophic factors and neurotransmitters[23]. Death of INL' cells was also reported in a previous study after exposure of the rats to white light[14, 26]. Accordingly, death of some cells of both ONL and INL could furtherly explain disruption of the outer plexiform layer (OPL) recorded in group II of the present study.

Retinal lesion induced by white PC LED light in this study could be assumed to be due to oxidative stress (OS). This assumption was supported by recognition of O_2^-, one of the reactive oxygen species (ROS), in group II compared to the undetectable value in the control rats (kept in complete darkness for absolute retinal recovery). This could be enforced by that OS was the essential cause of light induced retinal lesion detected formerly[27, 28]. Further reinforcement came from the recorded increase in total ROS level in the retina as early as 3 days after exposure to LED light[11].

Oxidative stress was reported to induce apoptotic photoreceptor cell death through the intrinsic pathway of apoptosis[11]. This might occur through release of cytochrome C from mitochondrial matrix[29] or excessive production of ROS from mitochondria after light exposure[30].

Group II of the current study revealed decrease in the number of ganglion cells in the ganglion cell layer (GCL) supported by the significant decrease in its mean number versus control group and the appearance of shrunken and irregular nuclei. This is consistent with what was reported in a previous study after exposure to fluorescent light[26]. Such finding could be explained by apoptotic ganglion cell death based on the presence of caspase-3 positive immunoreactivity in few cells of GCL. This explanation was enforced by that ganglion cells contained numerous mitochondria especially the unmyelinated intra-ocular part of their axons[31]. Moreover, GCL interacted with light before other nuclear retinal layers releasing ROS from the numerous mitochondria resulting into photo-oxidative apoptotic cell death[32].

Other essential finding reported in this study after white PC LED light exposure was the presence of multiple deeply stained glial cells within the GCL which was similarly reported previously[26]. This finding could be explained by that glial cells reacted to neuronal lesion by reactive gliosis (cellular hypertrophy with increased production of intermediate filaments and cellular hyperplasia) to support the injured neurons through production of neurotrophic factors. The glial cells in the retina included astrocytes in GCL and Müller cells in INL with their processes spanning the whole retinal layers[33, 34]. This explanation could be supported in the current study by the appearance of thickened Müller processes, preservation of inner limiting membrane (ILM) that was formed by the expanded ends of Müller processes, wide spread positive immunoreaction for vimentin, an intermediate filament, through retinal layers and the significant increase of its mean area percent in group II versus group I. This positive immunoreaction was extensively apparent in GCL indicating reactive astrocytes and INL indicating reactive Müller cells whose hypertrophied processes extending into IPL, GCL to ILM and into OPL and ONL (outer retina) towards the OLM. These findings are concomitant with what were stated by other researchers in a previous study[34]. It could be assumed that the extension of vimentin immunoreaction towards OLM occurred not only due to hypertrophy of Müller cells' processes but also due to proliferation and migration of Müller cells to replace the lost photoreceptors[34].

Inflammation was proved to be a common sequel associated with neuronal lesions such as retinal lesions and photoreceptors degeneration[35]. Thus, congested blood vessels found in GCL of group II in the current work could be explained by the inflammatory process associated with photoreceptors degeneration. Such inflammation occurred due to production of pro-inflammatory mediators as tumour necrosis factor-α (TNF-α), interleukin-1 (IL-1) by the reactive glial cells; Müller cells and microglia (one of the glial cells in GCL)[33, 34]. Production of TNF-α was reported to initiate inducible isoform of nitric oxide synthase (iNOS) expression by Müller cells and microglia[34]. This expression was supported in the present study by the positive immunoreaction for iNOS in GCL and INL in group II and its absence in control group. Increased iNOS led to increase production of nitric oxide, a reactive radical gas, resulting into more damage of the tissues by reactive nitrogen species[34].

Bearing in mind that the retina is one of the highly oxygen consuming tissues in the body and it has a large amount of membrane lipids especially in the outer segments where there are multiple membranes[36, 37]. So, in the presence of light energy, ROS might be generated within the retinal tissues and result into OS with subsequent photoreceptors degeneration. In addition, the retina is very sensitive to OS and contains an enzymatic system, especially in outer segment and RPE, which could protect against these ROS[11].

Thus, any imbalance between production of ROS and their neutralization by the protective retinal enzymes with increased release of ROS might lead to OS and photochemical photoreceptor damage[38, 39]. White PC LED light was recorded to have very high energy that generated high level of ROS much more than the protective capability of the retinal enzymatic system[2].

Photochemical retinal damage was proved to depend on duration of light exposure, light intensity and light wavelength (short wavelength led to more retinal damage)[24]. In the current work, there was normal exposure duration (normal dark/light cycle) and low intensity domestic light (750 LUX). So, retinal lesion induced by white PC LED was due to short light wavelength.

LED light was proved to emit higher level of short wavelength blue light than other traditional light[2]. Even white PC LED light that appeared white to the human eye was reported to progressively generate more blue light with gradual bleaching of phosphor and progressive decrease in its blue light absorption capacity[11].

Group II of the present study revealed features of cellular degeneration in RPE, in the form of shrunken deeply stained cells with shrunken irregular darkly stained nuclei. Such cellular degeneration could be explained by the most deleterious OS produced in the retina by the blue wavelength light which could result into death of the photoreceptor cells and their adjacent RPE cells. This extensive blue light induced OS resulted from shortening of the normal visual cycle

(rhodopsin is regenerated via long metabolic pathway in RPE). Such shortening occurred through formation of intermediate compounds that absorbed blue light and rapidly photoreversed to the original rhodopsin which in turn absorbed more light photons and caused more OS[40]. In addition, absorption of the blue light photons by retinal photo-pigment present in the outer segments resulted into formation and accumulation of A2E, an indigestible toxic compound[41]. A2E, in turn absorbed more blue light and generated more ROS. This extensive OS might lead to death of the photoreceptors and permanent visual loss[42]. RPE regularly engulfed the outer segments of the photoreceptors containing A2E and oxidative damage molecules and stored them in the form of lipofuscin pigment. Once these oxidative compounds were accumulated in RPE, they absorbed more blue light and led to more OS that might result into apoptotic cell death[43, 44].

This morphological retinal damage induced by the blue light emitted from the white PC LED sources was assumed to be followed by loss of the retinal function. This assumption was confirmed in a previous study[11] by significant changes in the electro-retino graph (ERG) in rats exposed to white PC LED when compared to that of the control rats (kept in darkness). They stated that loss of retinal neuronal functions might occur even if these neurons did not die where their death might not occur instantly after light exposure. Other researchers reported that if this light induced retinal lesion had occurred in the macula, it might predispose to and hasten AMD[2, 39]. This could be explained by that lipofuscin pigment limited the ability of RPE to support and provide nutrients to photoreceptors[45]. Moreover, RPE excreted these lipofuscin pigment into the sub-retinal space between RPE and Bruch's membrane forming drusen, the initiator of AMD[46]. Drusen accumulated in the macula interfered with nutritional supply of RPE resulted into their death[47] with subsequent death of the overlying photoreceptors due to lack of support and nutrition[48]. This was followed by the development of the dry form of AMD[49]. Furthermore, ROS, lipofuscin and drusen might lead to lesion of blood-retinal barrier with subsequent invasion of small blood vessels to the sub-retinal space. These blood vessels might break and/or leak resulting into haemorrhage and/or exudation and development the wet form of AMD[50].

In the present study, exposure of rats receiving nicotine (a model of chronic smoker) to white PC LED light revealed exacerbation of the retinal degeneration. This could be explained by that nicotine itself produced ROS and decreased the antioxidants[51] that aggravated OS produced by PC LED light. This was enforced in the current study by the significant increase in the mean value of O_2^- in group III versus group II. The striking increase in OS in group III of this study was suggested to cause marked apoptotic photoreceptor cell death either directly or indirectly through apoptosis of cells of RPE. Photoreceptors apoptosis was followed by death of cells of INL. Also extensive OS could result into marked apoptosis of ganglion cells[52, 53]. This suggestion could explain the presence of few cells within the layer of retinal pigmented epithelium which were either shrunken cells with pyknotic nuclei or swollen cells with absent nuclei and cytoplasmic vacuolations. It could also enlighten the presence of multiple empty spaces in both ONL and INL, cells with shrunken nuclei and cytoplasmic vacuolations in ONL, dark shrunken and irregular nuclei in INL and the significant decrease in ONL and INL thickness in group III versus group II. Additionally, it could elucidate the almost absence of OPL and inner and outer segments of PRL with marked disruption or complete absence of OLM. Moreover, it could clarify the presence of very few ganglion cells in GCL which were shrunken and irregular and the significant decrease in its mean number in this group compared to group II.

Although, apoptosis was assumed to increase in group III in ONL, INL and GCL, area percent of caspase-3 positive immunoreaction was significantly decreased in this group when compared to that of group II. This controversy might be revealed to phagocytosis of the apoptotic bodies which occurred as a normal sequence of apoptosis[54].

GCL of group III revealed the presence of multiple glial cells (Müller cells and astrocytes) that could be explained based on that massive retinal lesions extensively stimulated reactive glial cells to proliferate. Müller cells, the main retinal glial cells, also were extensively stimulated by severe retinal injury to proliferate and migrate invading the areas of lesions in all retinal layers and surrounding the entire retina by forming subretinal glial tissue. Such subretinal gliosis might aggravate the retinal lesion by blocking the blood supply from the choroid to the outer retina[25, 34]. This marked gliosis was supported in group III of the current study by the strong abundant positive vimentin immunoreaction that appeared extending through all retinal layers and replacing the disrupted OLM. Further support was achieved by the significant increase in its mean area percent in this group versus group II.

Extensive retinal lesion was accompanied by marked inflammatory process which is supported in group III of this work by marked congestion of the blood vessels in GCL. Such inflammation increased the recruitment of macrophages and monocytes in the choroid from where they invaded the outer retina (the main site of lesion) and produced iNOS[55]. This assumption was enforced by the extension of iNOS

positive immunoreaction in group III into the outer retina in addition to its presence in the inner retina with significant increase in its mean area percent in this group versus group II.

This deleterious white PC LED-retinal lesion aggravated by nicotine could accelerate AMD more than in case of retinal lesion due to light alone as nicotine was proved, in former study, to destroy carotenoids that protected the macula against light[56]. In addition to its damaging effect on RPE and its angiogenic effect on choroidal vessels leading to formation of choroidal neovasculature which occurred through stimulation of VEGF[12].

CONCLUSION

White PC LED sources are expected to be widely used for domestic illumination in the few coming years as it is the most effective and economic source of artificial lighting. It is also widely used in lighting of streets, factories, television, smart cellular phones and computer monitors. White PC LED light could result into deleterious retinal damage most probably through its higher blue light proportion with subsequent damaging oxidative stress than any other artificial light sources. This detrimental retinal lesion is markedly aggravated by smoking due to the toxic effect of nicotine, one of the main component of cigarette smoke, through production of ROS. Such retinal lesion may rapidly progress to AMD. Thus, caution should be taken during use of white PC LED light especially in cases of cigarette smoking.

CONFLICT OF INTEREST

There are no conflicts of interest.

ABBREVIATIONS:

Retinal pigmented epithelium (RPE), photoreceptor layer (PRL), outer segment (OS), inner segment (IS), outer limiting membrane (OLM), outer nuclear layer (ONL), outer plexiform layer (OPL), inner nuclear layer (INL), inner plexiform layer (IPL), ganglion cell layer (GCL), nerve fiber layer (NFL), inner limiting membrane (ILM), bipolar cells (B), Müller cells (M), Horizontal cells (H) and amacrine cells (A).

REFERENCES

1. Holzman DC. What's in a color? The unique human health effect of blue light. Environ Health Perspect. 2010; 118: a22–a27.

2. Behar-Cohen F, Martinsons C, Vienot F, Zissis G, Barlier- Salsi A, Cesarini JP, Enouf O, Garcia M, Picaud S, Attia D. Light-emitting diodes (LED) for domestic lighting: any risks for the eye?. Prog Retin Eye Res. 2011; 30: 239–257.

3. Spivey A. The mixed blessing of phosphor-based white LEDs. Environ Health Perspect. 2011; 119: 472–473.

4. Smith CJ, Hansch C. The relative toxicity of compounds in mainstream cigarette smoke condensate. Food Chem Toxicol. 2000; 38: 637–646.

5. Suńer I., Espinosa-Heidmann D., Marin-Casstano M., Hernandez E., Pereira-Simon S. and Cousins S. Nicotine increases size and severity of experimental choroidal neovascularization. Invest Ophthalmol Vis Sci. 2004; 45: 311–317.

6. Clemons T E, Milton R C, Klein R, Seddon J M, FerrisF. L. 3rd. Risk factors for the incidence of advanced age-related macular degeneration in the age-related eye disease study (AREDS), AREDS report no. 19. Ophthalmology 2005; 112: 533–39.

7. Davis SJ, Lyzogubov VV, Tytarenko RG, Safar AN, Bora NS, Bora PS. The effect of nicotine on anti-VEGF therapy in a mouse model of neovascular age-related macular degeneration. Retina 2012; 32: 1171–1180.

8. Wang A L, Lukas T J, Yuan M, Du N, Handa J T, Neufeld A H. Changes in retinal pigment epithelium related to cigarette smoke: Possible relevance to smoking as a risk factor for age-related macular degeneration. PLoS One 2009; 4, e5304.

9. Jain R K Clearing the smoke on nicotine and angiogenesis. Nat Med. 2001; 7: 775–77.

10. Heeschen C, Jang J J, Weis M, Pathak A, Kaji S, Hu R S, Tsao P S, Johnson F L, Cooke J P. Nicotine stimulates angiogenesis and promotes tumor growth and atherosclerosis. Nat Med. 2001; 7: 833–839.

11. Shang YM, Wang GS, Sliney D, Yang CH, Lee LL. White light–emitting diodes (LEDs) at domestic lighting levels and retinal injury in a rat model. Environ Health Perspect. 2014; 122: 269–276.

12. Kaliappan S, Jha P, Lyzogubov VV, Tytarenko RG, Bora NS, Bora P S. Alcohol and nicotine consumption exacerbates choroidal neovascularization by modulating the regulation of complement system. FEBS Lett. 2008; 582: 3451–3458.

13. El-Akabawy G, El-Kholy W. Neuroprotective effect of ginger in the brain of streprozotocin-induced diabetic rats. Ann Anat. 2014; 169: 119- 128.

14. Saenz-de-Viteri M, Heras-Mulero H, Fernández-Robredo P, Recalde S, Hernández , Reiter N, Moreno-Orduña M, García-Layana A. Oxidative stress and histological changes in a model of retinal phototoxicity in rabbits. Oxid Med Cell Longev., 2014; 2014: 1-10.

15. Kassan M, Montero MJ, Sevilla MA. Chronic treatment with pravastatin prevents early cardiovascular

changes in spontaneously hypertensive rats. Br J Pharmacol. 2009; 158: 51-57.

16. Kiernan J. Histological and histochemical methods: theory and practice. 3rd ed. London, New York & New Delhi: Arnold publisher; 2001. pp. 111-162.

17. Bancroft J, Gamble M. Theory and Practice of Histological Techniques. Staining methods. 7th ed. Edinburgh, London, Madrid, Melbourne, New York and Tokyo: Churchill Livingstone; 2008. pp. 263-325.

18. Hayat MA. Chemical fixation. In: Principles and techniques of electron microscopy: biological applications. 4th ed. Edinburg, UK: Cambridge University Press. 2000. pp.4–85.

19. Dykstra MJ and Reuss LE. Staining methods for semithins and ultra thins. In: Biological electron microscopy, theory, techniques and troubleshooting. 2nd ed. Kluwer Academic Publishers/Plenum Publishers. 2003. pp.175- 196.

20. Emsley R, Dunn G, White IR. Mediation and moderation of treatment effects in randomised controlled trials of complex interventions. Stat Methods Med Res. 2010; 19: 237-270.

21. Chepesiuk R. Missing the dark: health effects of light pollution. Environ Health Perspect. 2009; 117: 20–27.

22. Collier RJ, Wang Y, Smith SS, Martin E, Ornberg R, Rhoades K , Romano C. Complement deposition and microglial activation in the outer retina in light-induced retinopathy: inhibition by a 5-HT1A agonist. Invest Ophthalmol Vis Sci 2011; 52: 8108–8116.

23. Wasowicz M, Morice C, Ferrari P, Callebert J, Botteri1C V. Long-term effects of light damage on the retina of albino and pigmented rats. Invest Ophthalmol Vis Sci. 2002; 43:813-820.

24. Organisciak DT,Vaughan DK. Retinal light damage: mechanisms and protection. Prog Retin Eye Res. 2010; 29:113–134.

25. Hippert C, Graca AB, Barber AC, West EL, Smith AJ, Ali RR, Pearson RA. Müller glia activation in response to inherited retinal degeneration is highly varied and disease-specific. PLoS ONE 2015; 10: e0120415.

26. Gawish M, Azmy A, Abdallah M. Morphological study of retinal neurons after continuous exposure to fluorescent light in adult male albino rats. The Egyptian Journal of Histology 2011; 34: 459-469.

27. Dong A, Shen J, Krause M, Akiyama H, Hackett SF, Lai H. Campochiaro PA. Superoxide dismutase 1 protects retinal cells from oxidative damage. J Cell Physiol. 2006; 208: 516–526.

28. Lohr HR, Kuntchithapautham K, Sharma AK, Rohrer B. Multiple, parallel cellular suicide mechanisms participate in photoreceptor cell death. Exp Cell Res. 2006; 83: 380–389.

29. Remé CE. The dark side of light: rhodopsin and the silent death of vision the proctor lecture. Invest Ophthalmol Vis Sci. 2005; 46: 2671–2682.

30. Wood JPM, Lascaratos G, Bron AJ, Osborne NN. The influence of visible light exposure on cultured RGC-5 cells. Mol Vis. 2008; 14: 334–344.

31. Kroemer G. Mitochondrial control of apoptosis: an introduction. Biochem Biophys Res Commun. 2003; 304:433–435.

32. Godley BF, Shamsi FA, Liang FQ, Jarrett SG, Davies S, Boulton M. Blue light induces mitochondrial DNA damage and free radical production in epithelial cells. J Biol Chem. 2005; 280: 21061–21066.

33. Sarthy V, Ripps H. Role in retinal pathophysiology in: The retinal Muller cell: structure and function. 1st ed. New York: Kluwer Academic/ Plenum Publishers, US; 2001. pp. 181–216.

34. Albarracin R, Valter K. 670 nm red light preconditioning supports Muller cell function: evidence from the white light-induced damage model in the rat retina. Photochemistry and Photobiology 2012; 88:1418–1427.

35. Iandiev I, Wurm A, Hollborn M, Wiedemann P, Grimm C, Reme C E, Reichenbach A, Pannicke T, Bringmann A. Muler cell response to blue light injury of the rat retina. Invest. Ophthalmol. Vis. Sci. 2008; 49: 3559–3567.

36. Yu DY, Cringle SJ Retinal degeneration and local oxygen metabolism. Exp Eye Res 2005; 80:745–751.

37. Wang Y, Zhao L, HuoY, Zhou F, Wu W, Lu F, Yang X, Guo X, Chen P, Deng Q, Ji B. Protective effect of proanthocyanidins from sea buckthorn (hippophae rhamnoides l.) seed against visible light-induced retinal degeneration in vivo. Nutrients 2016; 8: 245.

38. Beatty S, Koh H, Phil M, Henson D, Boulton M. The role of oxidative stress in the pathogenesis of age-related macu¬lar degeneration. Surv Ophthalmol. 2000; 45:115–134.

39. Wu J, Seregard S, Algvere PV. Photochemical damage of the retina. Surv Ophthalmol. 2006; 51: 461–481.

40. Grimm C, Wenzel A, Williams T, Rol P, Hafezi F, Remé C. Rhodopsin-mediated blue-light damage to the rat retina: effect of photoreversal of bleaching. Invest Ophthalmol Vis Sci. 2001; 42: 497-50.

41. Shaban H, Richter C. A2E and blue light in the retina: the paradigm of age-related macular degeneration. Biol Chem 2002; 383:537-45.

42. Sparrow JR, Zhou J, Cai B. DNA is a target of the photodynamic effects elicited in A2E-laden RPE by blue-light illumination. Invest Ophthalmol Vis Sci 2003; 44: 2245-51.

43. Chen L, Dentchev T, Wong R, Hahn P, Wen R, Bennett J, Dunaief JL. Increased expression of ceruloplasmin in the retina following photic injury. Mol Vis. 2003; 30: 151-158.

44. Hammer M, Richter S, Guehrs KH, Schweitzer D. Retinal pigment epithelium cell damage by A2-E and its photo-derivatives. Mol Vis. 2006; 12: 1348-1354.

45. Nilsson SE, Sundelin SP, Wihlmark U, Brunk UT. Aging of cultured retinal pigment epithelial cells: oxidative reactions, lipofuscin formation and blue light damage. Doc Ophthalmol. 2003; 106:13-16.

46. Crabb JW, Miyagi M, Gu X, Shadrach K, West K A, Sakaguchi H. and Hollyfield J G. Drusen proteome analysis: an approach to the etiology of age-related macular degeneration. Proc Natl Acad Sci U S A. 2002; 99: 14682-14687.

47. Anderson DH, Mullins RF, Hageman GS, Johnson LV. A role for local inflammation in the formation of drusen in the aging eye. Am J Ophthalmol. 2002; 134:411-431.

48. Johnson PT, Lewis GP, Talaga KC. Brown MN, Kappel PJ, Fisher SK, Anderson DH, Johnson LV. Drusen-associated degeneration in the retina. Invest Ophthalmol Vis Sci. 2003; 44: 4481-4488.

49. Suter M, Remé C, Grimm C, Wenzel A, Jäättela M, Esser P, Kociok N, Leist M, Richter C. Age-related macular degeneration. The lipofusion component N-retinyl-N-retinylidene ethanolamine detaches proapoptotic proteins from mitochondria and induces apoptosis in mammalian retinal pigment epithelial cells. J Biol Chem. 2000; 275: 39625-39630.

50. Zhao L, Wang Z, Liu Y, Song Y, Li Y, Laties M A, Wen R. Translocation of the retinal pigment epithelium and formation of sub-retinal pigment epithelium deposit induced by subretinal deposit. Mol Vis. 2007; 13: 873-80.

51. Barr J, Sharma CS, Sarkar S, Wise K, Dong L, Periyakaruppan A, Ramesh GT. Nicotine induces oxidative stress and activates nuclear transcription factor kappa B in rat mesencephalic cells. Mol Cell Biochem.2007; 297: 93–99.

52. Dundar S, Ozcura F, Meteoglu I, Kara EM. Effects of long-term passive smoking on the vascular endothelial growth factor and apoptosis marker expression in the retina and choroid: an experimental study. Turk J Med Sci. 2012; 42: 377-383.

53. Ari S, Nergiz Y, Cingu KA, Atay EA, Sahin A, Çinar Y , Caca I. Effects of hyperbaric oxygen on crystalline lens and retina in nicotine-exposed rats. Cutan Ocul Toxicol. 2013; 32: 9-12.

54. Erwig LP, Henson P M. Clearance of apoptotic cells by phagocytes. Cell Death and Differ. 2008; 15: 243–250.

55. Ng T F, Streilein J W. Light-induced migration of retinal microglia into the subretinal space. Invest. Ophthalmol. Vis. Sci. 2001; 42: 3301–3310.

56. Czaplicka E, Grabska-Liberek I, Rospond I, Kocięcki J. Environmental exposure to tobacco smoke and condition of organ of vision. Postępy Nauk Medycznych, t. XXVI, 2013:865-867.

الملخص العربى

دراسة هستولوجية علي الآثار الضارة لضوء الليد الأبيض على شبكية عين الجرذان البيضاء البالغة والتأثير المحتمل لتزامن تناول النيكوتين معه مع القاء الضوء على آليتهم الممكنة

إيمان عباس فرج، مروة محمد يسري، عبير إبراهيم عمر
قسم الهستولوجيا ـ كلية الطب ـ جامعة القاهرة

الخلفية: اثبت الثنائي الباعث للضوء (الليد)، مصدر الضوء الصناعي الأكثر فعالية والاقتصادي انه باعث للضوء الأزرق أكثر من المصادر التقليدية للضوء حتى من ضوء الليد الأبيض الأكثر انتشارا. للضوء الأزرق العديد من المشاكل الصحية مثل تلف الشبكية الضوئي. النيكوتين، واحد من المواد الصلبة الرئيسية لدخان السجائر، والمتسبب في تلف نهائي للأعضاء والمحفز لتلف الشبكية من خلال آليات مختلفة.

الهدف من العمل: بحث التغييرات المحتملة في شبكية العين الناجم عن ضوء الليد الأبيض المستخدم في المنازل في الجرذان البيضاء، والتأثير المحتمل للنيكوتين على هذه التغييرات والقاء الضوء على آليتهم الممكنة.

المواد وطرق البحث: تم تقسيم اثنان واربعين من ذكور الجرذان البيضاء البالغة بالتساوي إلى ثلاث مجموعات: الضابطة (I)، الليد(II) والنيكوتين-الليد (III). وظلت كلا من المجموعة الثانية والثالثة لمدة ٥ أيام في الدورة العادية الضوء / الظلام ، ١٤ يوما من الظلام ، ثم الدورة العادية مع ضوء الليد الأبيض لمدة ٩ أيام. بالإضافة إلى ذلك، تلقت جرذان المجموعة الثالثة النيكوتين يوميا عن طريق الفم (٣ ملجم / يوم) لمدة ٢٨ يوما (مدة التجربة).

تم تشريح جميع الجرذان في نهاية التجربة وتم قياس مستوى الأكسيد الفائق (O_2^-) في خليط الشبكية لكل مجموعة. خضعت قطاعات الشبكية لجميع المجموعات لصبغة التولودين الزرقاء، الهيماتوكسلين والإيوسين والصبغة الهستوكيميائة المناعية للكاسباس ٣، ڤيمنتين وأكسيد النيتريك سينسيز المستحث (iNOS). وقد تم قياس المساحة المئوية من ردود الفعل الإيجابية بالإضافة إلى سمك طبقة الانوية الخارجية والداخلية وعدد خلايا العقدة العصبية ثم حللت إحصائيا.

النتائج: تم الكشف عن مظاهر لتلف الشبكية وزيادة مستوى الأكسيد الفائق في كلا من المجموعتين الثانية والثالثة وكان التلف بالغ في المجموعة الثالثة. واظهرت الدراسة الهستوكيميائة المناعية للمجموعة الثالثة عن ردود فعل ايجابية ذات زيادة ملحوظة في ڤيمنتين وا.ن.و.س وانخفاض كبير في كاسباس ٣ مقابل المجموعة الثانية.

الخلاصة: يمكن أن يؤدي ضوء الليد الأبيض إلى تلف بالغ للشبكية والذي يمكن أن يزداد سوءا بالنيكوتين، المكون الرئيسي لدخان السجائر، وقد يتطور سريعا إلى الضمور البقعي المرتبط بالعمر.

الكلمات الرئيسية: الليد، النيكوتين، الشبكية، ڤيمنتين، iNOS وكاسباس ٣.